Design and Simulation of an Electromagnetic Aircraft Launch System

(*) D Patterson, A Monti, C Brice, R Dougal, R Pettus
(**)T Bertoncelli
(*) Department of Electrical Engineering - University of South Carolina
Swearingen Center – Columbia, SC 29208 USA
Phone: +1 803 7777362; Fax: +1 803 777 8045
E-mail: patterson@ieee.org
(**) Dipartimento di Elettrotecnica – Politecnico di Milano
Piazza Leonardo Da Vinci, 32 – 20133 Milano – Italy
Phone: +39 02 23993702; Fax: +39 02 23993703
E-mail: tiziana.bertoncelli@etec.polimi.it

Abstract

This paper describes the basic design, refinement and verification using finite element analysis (FEA), and operational simulation using the Virtual Test Bed (VTB), of a range of candidate linear machines for an electromagnetic aircraft launching system (EMALS) for the aircraft carrier of the future. Choices of basic machine format, and procedures for determining basic dimensions are presented. A detailed design is presented for a permanent magnet version, and a super conducting field coil and an induction machine version are introduced. The long armature – short field geometry is discussed, and in particular the impact of this geometry on the scale of the power electronic drive system is presented.

1 Introduction

1.1 The Project

Modern ship designs are increasingly moving towards the use of electricity to distribute, control, and deliver energy for the multiplicity of on board needs. This trend has already resulted in large direct drive electric machines for traction in commercial shipping. In some significant cases, including traction, adoption in military applications is rather slower, because of the comparatively low achievable power, energy and torque, per unit volume and per unit mass, of electro-mechanical energy conversion systems.

However the benefits of controllability, robustness, reliability, damage management, operational availability, reduced manning etc. are undeniable. Whilst all actuation systems are under continuous investigation, there is a high level of interest in determining the feasibility an electromagnetic aircraft launch system (EMALS) for the aircraft carriers of the future.

Studies are being carried out at the University of South Carolina (USC) to investigate possible competing solutions and to determine their feasibility and comparative strengths. Simulation uses the Virtual Test Bed (VTB), a new environment for simulation and virtual prototyping of power electronic systems that includes not only simulation of system dynamics, but also solid modeling of the system and visualization of the system dynamics. To fully accommodate the breadth of disciplines that power electronics encompasses, the VTB provides several advanced capabilities, including

- *Multiformalism* – the ability to express in different languages the models of the various components that make up a system,
- *A highly interactive environment* – wherein users can change the system topology or parameters while a simulation executes, and

- *High-level visualization* -- which aids the user to rapidly comprehend the system performance [1].

EMALS also represents a challenging test case for VTB itself. Models of the different parts of the systems will be built up from the specifications and the characteristics given by U.S. Navy, and from engineering design principles.

1.2 The Challenge

The design of an EMALS has many intriguing challenges. The likely specifications and technical features include:

Maximum velocity:	200 kt	~100 m/s
Maximum power stroke:	310 ft	~100 m
Min braking distance - moving member	30 ft	~10m
Maximum Energy:	120 MJ	
Maximum Thrust	1.3 MN	
Minimum time between launchings	50 s.	

A typical launch might be for a 25000 kg aircraft accelerated to 150 kt in 2.7 s, at an acceleration of 2.8 g. This represents a total energy of 70 MJ. Acceleration to the maximum velocity (higher than the typical velocity) requires a more-challenging 2 s stroke, at a constant acceleration of 5 g.

Whilst the overall system design must include storage, power electronics, and control system design, this paper will concentrate on the electric machine design, and introduce some of the power electronics and control issues.

2 Linear Machine Design

2.1 Background

A substantial body of research exists studying large linear motors, however the majority of these are induction machines, and by far the largest number of these are what are known as short primary - long secondary machines. We will also use the terminology short armature - long field for this geometry, a little more apt for machines other than induction machines. Significant issues in design of these machines are the study of edge effects and end effects [2] [3] [4] [5] [6] [7].

A very common application of short primary long secondary machines is for traction in electric trains, where the energy is delivered to the train via a catenary or third rail system, and applied to an on board armature or primary. The secondary, or field member, is some form of complete track length reaction rail. The Westinghouse “Electropult”, developed during World War II is an aircraft launching linear induction machine of this form [8].

The EMALS project at USC is examining an extensive range of possible electrical machines, induction machines, permanent magnet (PM) machines, and machines with super conducting coil field structures. The issue of the transfer of >120 MJ in 2 seconds to a moving member, (referred to hereinafter as the shuttle) either through sliding contacts or some form of moving harness, is daunting. The “Electropult” referred to above used sliding contacts; however, the thrust required for this EMALS project is about 20 times greater than that delivered by the Electropult. An historical description of the Electropult says, “…the operational costs were so high that in spite of the encouraging performance, steam catapults held the field” [9]. The simplicity of the dc motor driven flywheel and the linear induction machine with a flat “squirrel cage” stator lead one to the conclusion that the operational costs must have been almost totally associated with the sliding contacts.

The need to decelerate the shuttle also makes minimization of shuttle mass a strong design constraint. These factors, together with the limited length of travel, have lead to the initial study of long primary - short secondary, or long armature - short field machines.

2.2 Basic Machine Sizing

Initial sizing of any machine is often done by considering "Electromagnetic Shear Stress", as defined in Fig 1. Miller quotes numbers for typical machines as being between 0.7 and 2 kN/m^2 for fractional horsepower induction machines ranging up to between 70 and 100 kN/m^2 for very large liquid cooled machines such as turbine generators, adding that peak rating may exceed these values by 2 to 3 times [10].

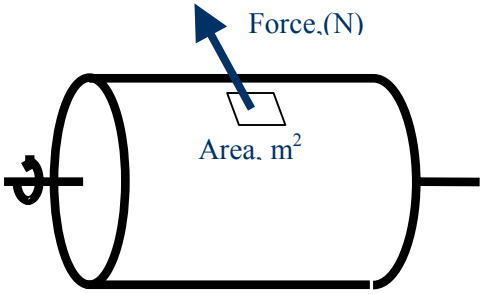

Fig 1. Electromagnetic Shear Stress Definition.

The Electropult, which can be considered as an induction machine with variable resistance "rotor", operated at a stress of a little greater than 50 kN/m^2. This makes sense for a machine which was highly inefficient, spending most of its operational time at a slip of greater than 50%.

It is worth noting that at 100 kN/m^2, for the aircraft launch system to produce 1.29 MN, the active area of the shuttle would need to be in the order of ~13 m^2, or 6.5 m^2 per side in a double sided structure. Early calculations were based on structure of roughly this size, attempting to keep the moving mass in the order of 1 tonne. (1 tonne at 100 m/s has 5 MJ of kinetic energy). The permanent magnet design presented below operates at 200 kN/m^2, and the superconducting field coil machine coil at 400 kN/m^2.

Similarly electric machine design is driven by current ratings in conductors. Under intermittent loading maximum workable current densities are between 30 and 50 A / mm^2.

2.3 Basic Machine Format

In order to achieve the surface area determined by achievable stress figures, two geometries were considered, the "inverted U" and the "blade" as shown in Figs 2 and 3.

Whilst for the inverted U the overall machine will be lighter, the mass of the shuttle must include material for completing the magnetic circuit. There are also issues with supporting the single winding structure and thermal management of a narrow vertical structure. In contrast, the blade structure allows the lightest possible shuttle, and a total mass of the two-sided stator which is within the design goal mass, and also has very good thermal paths. Thus the blade structure has been chosen for this design study.

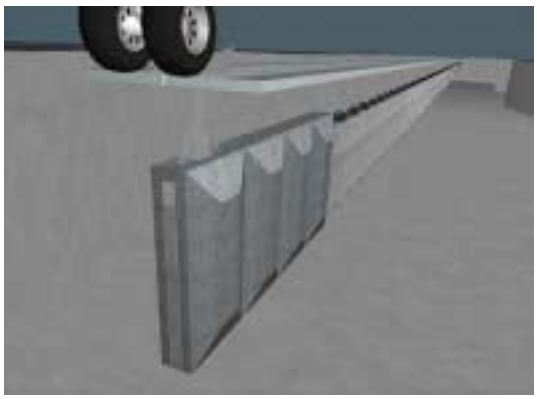

Fig 2. Inverted U shuttle

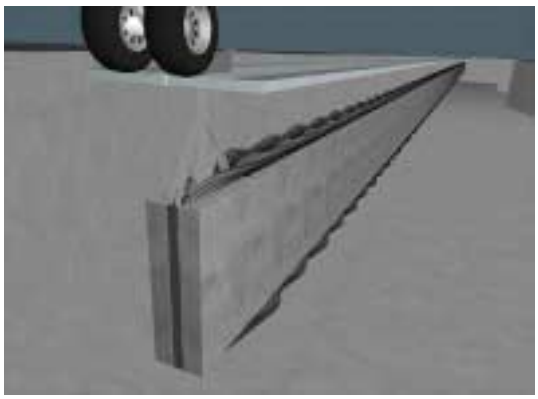

Fig 3. Blade shuttle

2.3.1 Pole Pitch

A very significant determinant of machine general performance is that of the pole pitch. Short pole pitches usually lead to higher efficiencies (less end turn length), thinner back iron on the stator sections, important for total mass, and are usual in high torque / force machines of large size. Limitations on indefinite reduction of the pole pitch have to do with the fundamental frequency of the drive power, which is also the frequency of flux reversal in parts of the magnetic structure resulting in core loss, and fringing effects between adjacent poles, which are related to the achievable minimum air gap. A pole pitch of 150 mm is currently under consideration, which results in a maximum frequency of 333 Hz in the magnetic circuit of the synchronous versions of the machine.

2.3.2 Stator, Slot Dimensions

It has been shown that at least for surface PM machines, eddy current loss in the stator teeth is proportional to the number of slots per pole per phase [11]. At the minimum one slot per pole per phase, with a traditional overlapping winding, a stator as shown in fig 4 has been dimensioned for initial FEA study.

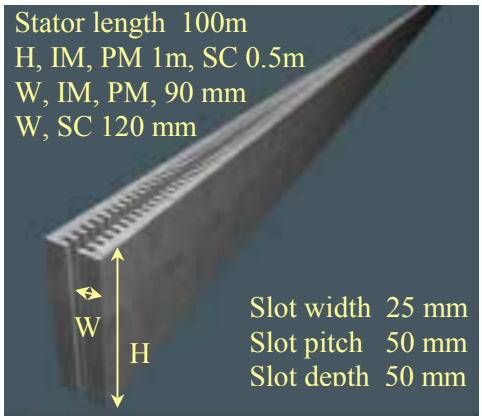

Fig 4. Stator Dimensions

The steel of the PM and induction stator has a total mass of 100 tonnes, and for the super conducting version 75 tonnes. The max allowable total system mass in the design specification is 530 tonnes, and the goal mass is 270 tonnes, so these structures are comfortably inside these specifications. The thermal mass of the 100 tonne structure is such that an energy dump of 40 MJ, for a very inefficient machine, will result in less than one degree Celsius temperature rise per shot. Thus active cooling will not be necessary.

As will be seen below, the inductance of the winding is a primary determinant of the complexity of the power electronic drive system, so that the stator is designed with open slots to minimize winding inductance. The stator winding scheme, using the traditional three phases, which is not obligatory, but gives a good starting position for a first design, is as summarized in figure 5.

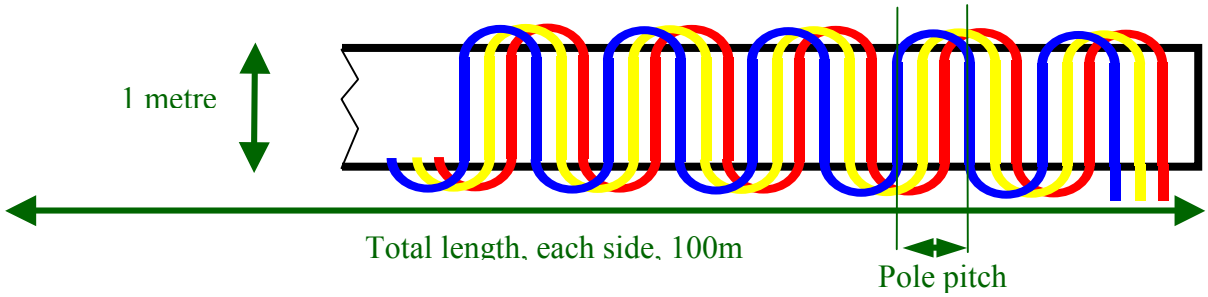

Fig 5. 3 phase, 1 slot per pole per phase, stator winding (armature) structure.

2.4 Driving the Armature

Using the permanent magnet machine stress of 200 kN/m^2 as discussed above, yields a shuttle length of 3 metres. Assuming standard 6 step servo drive, a pole pitch of 150 mm, an achievable flux density in the air gap of 0.9T, and a total thrust of 1.29 MN, a slot current of 18 kA, (from f = bli), results.

If this is in a single conductor in the slot, of 20 * 40 mm (64% fill factor), a current density of 22.5 A/mm^2 results, yielding an estimated total copper loss of 2.2 MW for the complete launcher. Since the machine rating is 61 MW the efficiency, considering copper loss only, is thus over 96%.

The more important issue is that, confirmed by FEA, the inductance of the single conductor in the slot is 2.6 □H/metre. Of course the single conductor can be divided, reducing the individual conductor current and the switch current, using more than 1 turn for the winding without affecting the copper loss (providing the same fill factor results) but the inductance goes up as the number of turns^2.

Even at 1 turn, the inductance of a single phase 200 metres in length for both sides, pole pitch 150 mm, without considering end turns (where the inductance is negligible, not being in iron) computes to 3.5 mH. In order to commutate from +18 kA to –18 kA at 333 Hz rate a voltage bus of 250 kV would be required. Clearly driving the track in sections is the only feasible option.

2.5 Simulation

Discussion so far has indicated the very large range of possibilities that need to be compared and considered when conceiving of a system of this level of complexity. Most commonly, promising research directions are deduced from data from existing operation systems. Without operational systems to guide research, recourse must be had to very powerful cross-disciplinary system simulators.

2.5.1 VTB

VTB is an ideal tool to explore the very broad range of combinations of the many possible variants for an EMALS, and to be able to converge on optimal systems. The project is enabling experience in machine design and simulation to be applied to a very detailed study focusing on a range of important criteria including total system mass, total system volume, thermal management, reliability, robustness, survivability via redundancy, and also acoustic, magnetic, and electromagnetic signatures of this very large pulsed power application.

3 Detailed Machine Design

In this research project, the majority of effort has so far been directed to the permanent magnet version of this machine, which has resulted in as surprisingly simple and achievable design. Some effort has been expended to explore the super conducting field coil version, which has some intriguing implications, and less effort on the induction version, since this is an area where a substantial body of expertise exists. Each of the three types is considered separately below.

4 Permanent Magnet Machine

At the pole pitch of 150 mm discussed above, a 3 metre shuttle would involve some 20 blocks of Neodymium Iron Boron (Nd Fe B) magnet material, supported in a composite structure. The magnet thickness is determined by 2 things,

(a) the achievable airgap and the design requirement of near to 0.9T in that airgap, and
(b) the requirement that the magnet is not demagnetized by the slot current of 18 kA

The design analyzed uses an airgap on each side of 5 mm, and a total magnet thickness of 100 mm. Using 120□magnet widths, the total magnet mass for the shuttle computes to 1480 kg. At 100 m/s, and increasing the mass by 10% for the supporting composite structure, the shuttle has a kinetic energy of 8.14 MJ. Using the same winding scheme as for launching, producing a reverse thrust of 1.29 MN, this shuttle can be stopped electrically, with full energy recovery, in 6.3 metres, well inside the allowed distance of 10 metres.

4.1 Finite Element Analysis

2D FEA has been used to verify certain aspects of the design, and to make refinements.

4.1.1 Demagnetization

The shuttle with 120□(100 mm) magnet widths, and 20 poles of alternating polarity, begins and ends with a half width magnet. For simplicity in modeling, the analyzed shuttle had 5 poles, beginning and ending with a half, and with 4 complete poles, as shown in figure 6. Note that only half of the geometry is entered, invoking symmetry around a centre line. Thus the drawing is of a top view of one side of a short section of the complete machine.

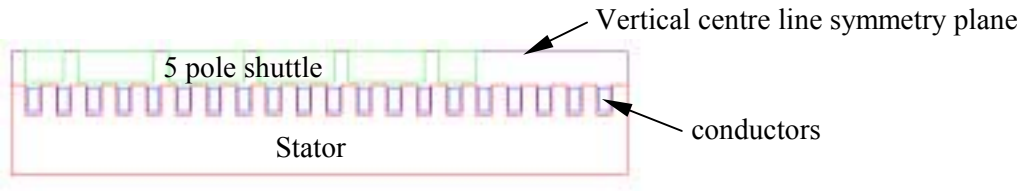

Fig 6. Geometry used for FEA

This model was analyzed for the vertical component of B in the magnets with 18 kA in the conductors, at a range of horizontal positions of the shuttle. At each position the field plot was checked to ensure that the B was reduced by less than 80%, since at 100% reduction, permanent demagnetization occurs.

4.1.2 Thrust Linearity

Rectangular magnets and open slots as shown above are capable of developing very substantial cogging forces, which themselves are indicators of variation in permeability which result in increased iron loss, due to flux ripple. The magnet width can be adjusted to control this cogging force, usually at the cost of increased ripple in the back emf. In this intermittent duty machine iron loss is not a serious issue, however any thrust ripple adds extra unwanted stress to the airframe. Whilst thrust ripple can be controlled by current control, the option to minimize thrust ripple, without considering cogging force, by adjustment of magnet width, was exercised with surprisingly effective results.

Figure 7 shows the thrust as a function of position with two windings energized with constant current, as is usual with simple 6 step switching. Since each phase will be independently controlled, handover at the edges of the 60□section can be managed to provide a smooth transition from one phase pair to the next.

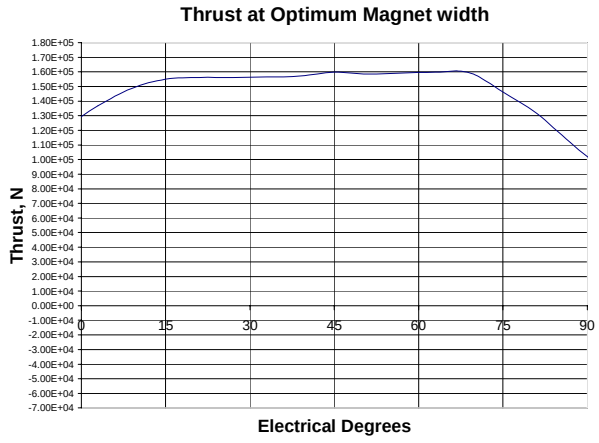

Figure 7 Thrust determined by FEA for constant current in two phases, as a function of shuttle position in electrical degrees

4.2 Power Electronics

Whilst the machine design turns out to be surprisingly simple, the power electronics design, particularly with the long armature – short field geometry is challenging, and very much dependent on the ratings of available switches. As discussed above in section 2.4, the track must be sectioned into driveable lengths. In order to provide a high level of control, to provide high levels of redundancy, and to provide the option to use other than three phases, it was decided to drive each separate phase winding in each section independently, with its own H bridge.

4.2.1 Typical Devices

A very promising device, and one for which USC has been developing models, is the IGCT. One of the principal models developed is for a device with a rating of 4 kV and 2.4 kA. Two of these in parallel can be used as a switch element to make an H bridge with 4 kV 4.8 kA ratings. This configuration has been adopted for the early simulations. In order to manage 18 kA in each slot, It was decided to use 4 independent turns in each phase, each with its own H bridge, so that in any section of the track. 3*4=12 H bridges are required.

4.2.2 Sectioning the Track

At every point along the 100 metre track a maximum driveable inductance can be calculated, based on the maximum possible velocity at that point. For example, at the end of the track the maximum velocity is 100 m/s. The □I is from - to + 4.8 kA, or 9 kA, the □T is, from the velocity and the pole pitch = 0.5 ms, the E manageable by the bridge is 4 kV, resulting a in an $L_{max,\ 100\ metres}$ of 0.22 mH.

This inductance results from both sides of 5 metres of track for a single turn of a single phase. Thus the final section of the track to be driven, given the available switches, can be only 5 metres in length.

Designing backwards from the end of the track results in 12 sections, increasing from 5 to 15 metres for the initial section.

At first it might seem that this implies, at 12 H bridges required to drive a 4 turn 3 phase section, a grand total of 144 H bridges; however, it is obvious that no more than 2 sections are ever activated at the one time, since the shuttle at 3 metres is shorter than any section. Therefore in operation, section 1 of the track is activated, and the shuttle begins to move. As the leading edge of the shuttle arrives at the start of section 2, section 2 is activated as well, and then as the trailing edge of the shuttle leaves section 1, section 1 is deactivated, The H bridge set that was driving section 1 can be disconnected from section 1, and connected to section 3 in readiness for the arrival of the leading edge of the shuttle at the start of section 3.

4.2.3 Power Electronics Switching Matrix

Thus a workable switching matrix involves 2 sets of 12 H bridges. Connection of each bridge in a set to one of 6 sections, (one set drives sections number 1,3,5,7,9, and 11, the other set drives the even numbers) can be done using back to back thyristors, which would be continuously triggered when required, and will switch off when the current decays to zero, when the H bridge switches are no longer driven. There is adequate time in all cases for this to happen. Figures 8 and 9 show the overall matrix structure, and the H bridge – thyristor connections, respectively.

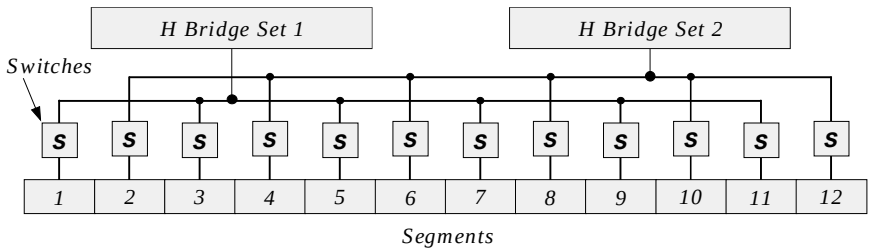

Figure 8. Overall Switching Matrix Structure

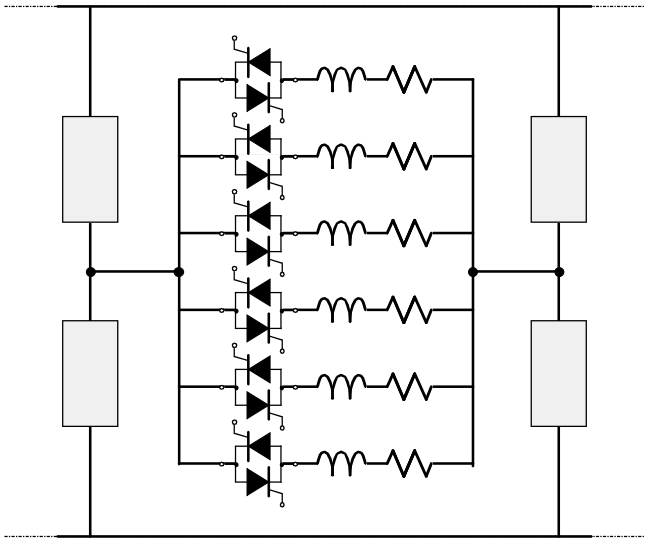

Figure 9 The H – Bridge - Thyristor - Winding connection

4.3 Overall System Design

As a part of the overall EMALS project, a design validation is being carried out via a high level simulation. The goals of the design validation are to

- Identify and define the EMALS high-level organization and subsystems.
- Create a high-level simulation that implements the interaction of the major EMALS subsystems through the use of behavioral models based on the EMALS describing equations. This simulation

  (1) provides a framework for formalizing the high-level describing equations and a mechanism for validating the behavior of the system and

  (2) helps to identify critical interactions and subsystem requirements.

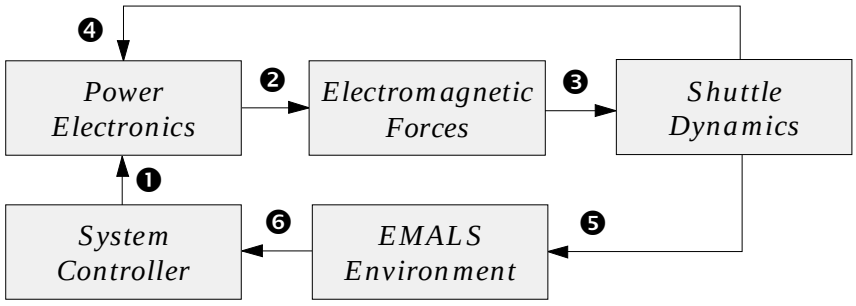

Figure 10. EMALS organization and major subsystems

The resulting high-level structure is show in figure 10 above. The subsystems defined are:

- *EMALS Environment* – Implements all of the mechanical dimensional characteristics and provides the mechanical coordinate system. Given the location of the shuttle, the environment provides the values (position) needed to control the H-bridges, both by segment and by phase. *Input* (❺): Shuttle position and speed (and indirectly, the sensors that provide this information). *Output* (❻): Shuttle position relative to the stator, as reported by the sensors.
- *Power Electronics* – The power supply and the H-bridges. *Inputs* (❶): Set points from the controller (per bridge) and indirectly, the load characteristics of the motor (EM forces block). *Output* (❷): Current through the stator windings.

- *Electromagnetic Forces* – Determines the force acting on the shuttle. This subsystem represents the EMALS linear motor. *Input* (❷): Amount of current through each stator winding. *Output* (❸): Force on the shuttle.
- *Shuttle Dynamics* –Provides the speed and location of the shuttle. *Input* (❸): Force acting on the shuttle. (The aircraft load is reflected to the shuttle and represents an indirect input.) *Outputs* (❹): Shuttle position to the environment. (❺) back EMF to the power electronics. The back EMF is computed here since it requires both the coefficients from the motor and the speed of the shuttle.
- *System Controller* – Switches the H-bridges and determines the set point current for each bridge. *Input* (❻): Location of the shuttle within the environment. *Outputs* (❶): Set points to the h-bridge controllers.

In addition to providing a mechanism for validating the design concept, the high-level simulation provides design constraints for the individual subsystems.

4.4 VTB Simulation

The authors are currently developing models for all of the individual system components. Some preliminary simulation results are already available as well as a simulation-driven animation of the 3D system showing the obtainable performance. Effort is currently being concentrated on the permanent magnet brushless motor case.

4.4.1 Machine modeling

A standard d-q model was developed for such a machine [12]. In order to replicate the modularity of the motor in the modeling structure an original approach to the model formulation was adopted.

The model architecture has two separate parts:

- The stator winding model
- The shuttle model

The system is designed so that any set of independent stator section models can be connected to a single shuttle.

The stator model represents the current in a single winding and it defines the force contribution of that stage to the overall system force.

The superposition theorem is applied in the shuttle model to sum the force generated by each section and then to solve the mechanical equations for speed and position. This information is sent back to the stator sections in order to evaluate the electromotive force.
The equivalent circuit of the stator model is illustrated in Figure 11.

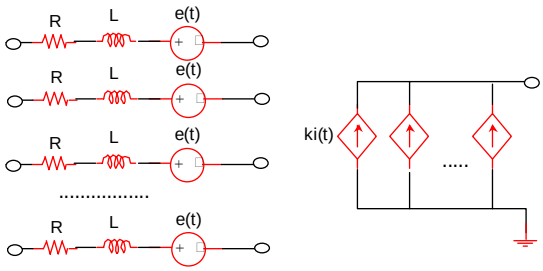

Figure 11: The equivalent circuit of the stator model

Each winding is represented with its equivalent circuit: considering that the design suggested 4 turns for each phase, the model is able to represent 12 independent circuits for any single section.

The evaluation of the electromotive force and the mechanical force coefficient is based on the mechanical position and velocity. First of all a check is performed to evaluate if the shuttle is over the section, so that the action of the permanent magnet is present, and then a check of the position within the section determines the specific values.

The mechanical system is modeled through the equivalent circuit shown in Figure 12.

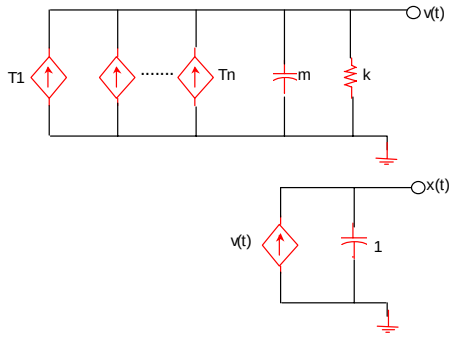

Figure 12: The equivalent circuit of the mechanical part

In this circuit we have two separate sections: the speed calculation obtained by summing the force from all the sections and the position calculation obtained as a pure integration.

A set of tests were performed to validate the modeling approach. The results of the first test are illustrated in Figure 13.

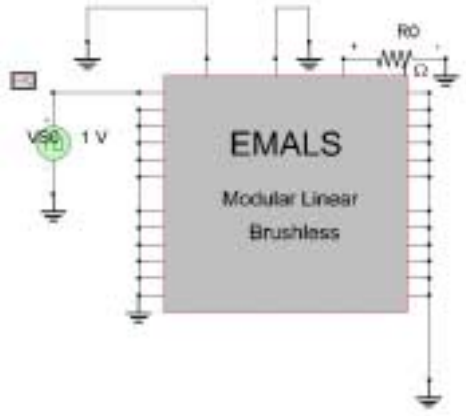

Figure 13 A first simulation test

The pins on the sides are the electrical terminals, while those on top are for the mechanical interface. In this case the speed and position are fixed to zero (the two pins on top are grounded – equivalent to a locked-rotor test), while a square wave voltage feeds one winding. This test verifies the correctness of the electrical subsystem and a classical R-L transient is the computed result (see Figure 14).

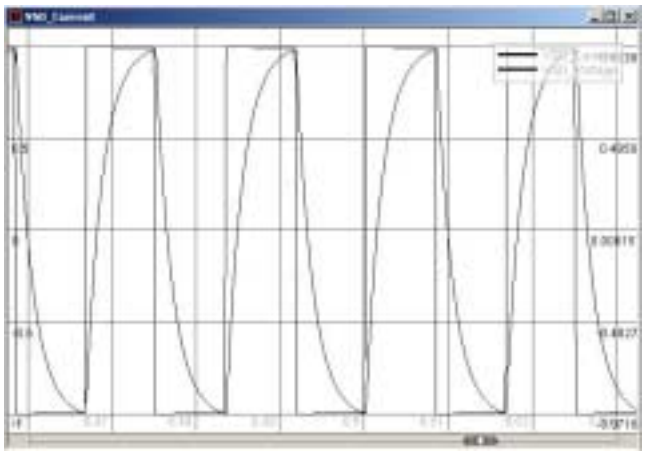

Figure 14. The results of the first test

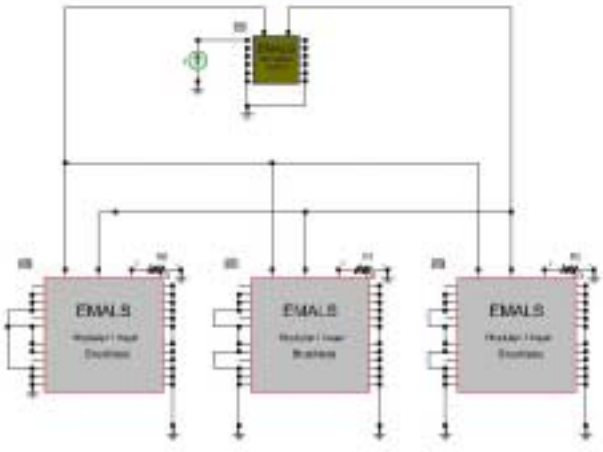

Figure 15 The second test

A second test as described in Figure 15 validated the mechanical model. In this case we have three stator section models and one shuttle model. A force is applied to the shuttle and then we measure the voltage across the open-circuited stator electrical windings. In this case we see the classical trapezoidal waveform that appears only for those sections that are under the shuttle (see Figure 16).

4.4.2 Converter modeling

All the switching alternatives are considered. A completely separate drive circuit for each coil is seen as the best solution, and as suggested above the ideal energy storage system may well consist of an energy storage unit for each bridge circuit. Averaged models of PEBB-like converters have been used to speed up the simulation; but switched versions also can be used.

In the first simulation an H bridge configuration for each phase was adopted: This means that a single converter was connected in parallel to 4 different windings. Since we are using ideal switch models at this stage, this is a reasonable thing to do.

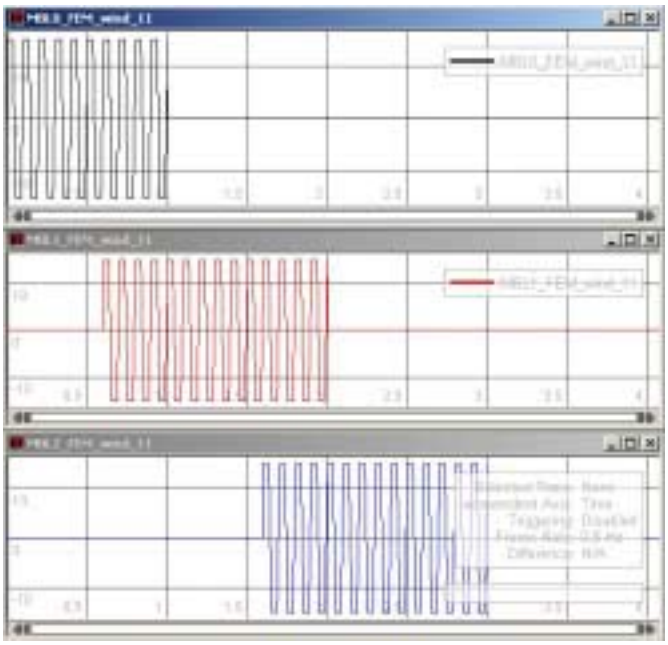

Figure 16. The results of the second test

4.4.3 Control modeling

The controller was modeled by using the VTB-Simulink interface. The controller is designed to fulfill the following requirements:

- each independent coil is fired by shuttle position sensors located along the stator.
- preset current (thrust) levels in each coil are known.
- open loop operation is possible if communication fails or is damaged.
- If communication exists, each coil thrust is adjusted as it is firing, so as to ensure adherence to the required thrust/ velocity profile.

The control algorithms are designed in Simulink, tested interactively, and finally compiled for better simulation performance.

The modular structure of the motor requires a hierarchical structure for the speed control.

Only one speed control (System Manager or SM in the following) is used, and as many current controllers as the number of H bridges (Hardware Manager or HM in the following). According to the position, the SM will decide which sections have to activate the current control.
Figure 17 shows the structure of the SM. A simple PI control performs the speed control task while the reference for each section is generated by a “section selector” block. Each HM receives a current reference and implements the current strategy as shown in Figure 18.

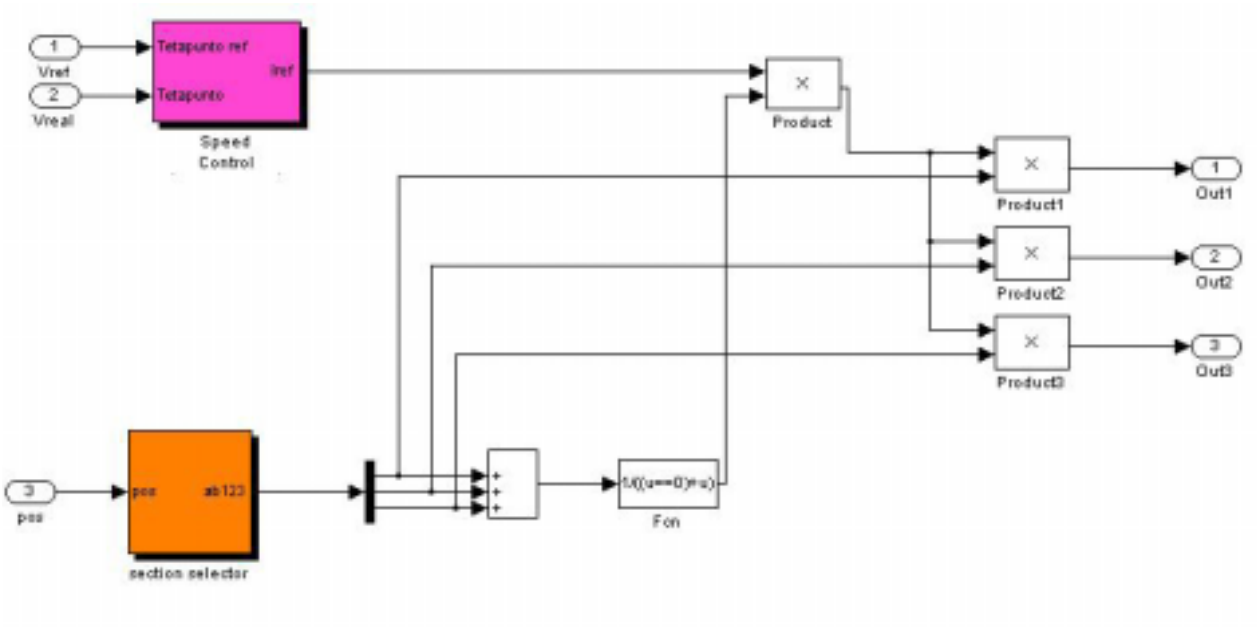

Figure 17. The SM structure in Simulink

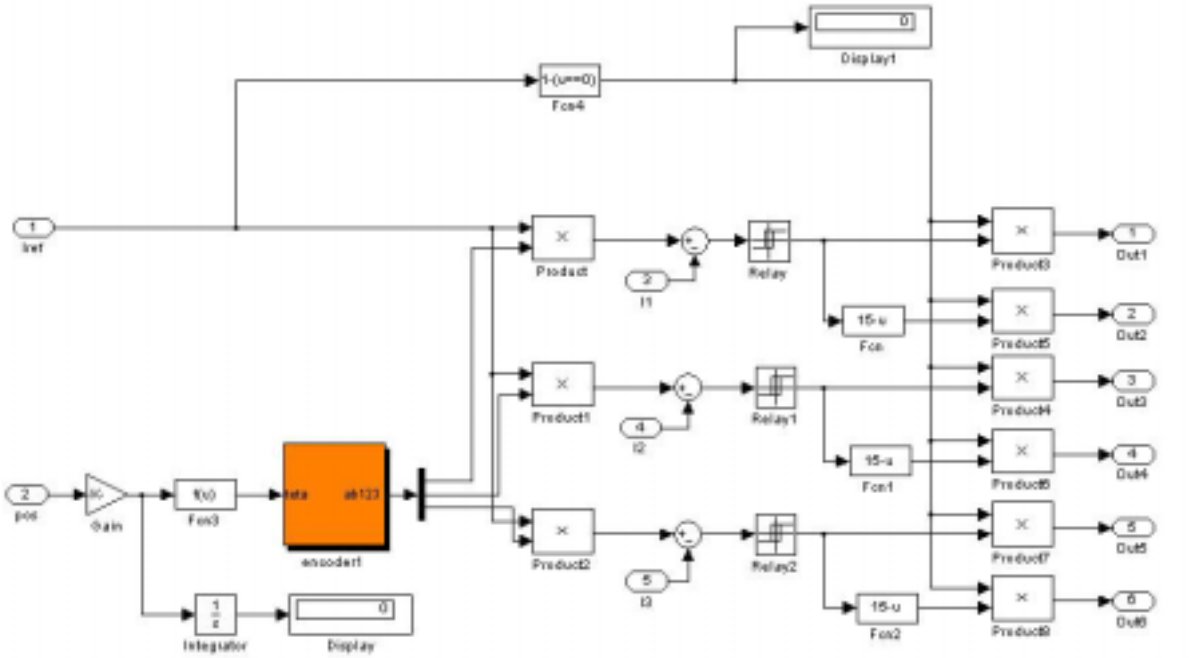

Figure 18. The HM structure in Simulink

Figure 19 shows part of a simulated aircraft launching event. The waveform represents the current in one of the windings of the first section. At the beginning the current ramps up and the control performs the classical square waveform. After a while, the shuttle leaves the first section and the current reference is set to 0.

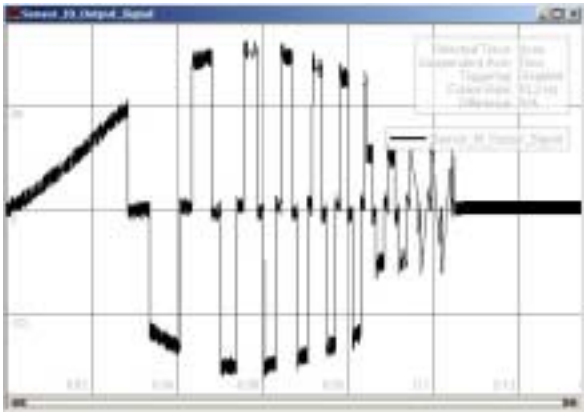

Figure 19 Current during the starting transient for first section

4.4.4 3D Visualization

In parallel with the mathematical development of the model, a 3D view of the system was implemented in the Visualization eXtension Engine of VTB (VXE). This allows for interesting system analysis, and will be especially valuable when the whole system model is completed. An example of a close view is shown in Figure 20.

Figure 20: A single frame from an animation of the EMALS system showing one side of the stator only.

5 Super Conducting Field Coil Machine

Work to date has involved the FEA modeling of a system with the stator dimensions discussed in section 2.3.2. Initial runs have been carried out using a one turn field current of 250 kA, which produces ~2T in the airgap, so that the back emf per section is exactly as for the PM machine, and the same currents produce ~twice the shear stress, and therefore the same total thrust. Since the inductance is halved, by halving the conductor lengths, the track sectioning is reduced significantly. Further work will optimize the coil width, and examine the need for stranding in the copper conductors. Stranding may well be necessary since tooth saturation will force flux into the conductors, resulting in high eddy current loss in the copper.

6 Induction Machine

Following the completion of the superconducting field coil machine analysis a more traditional induction version will be designed, analyzed, and simulated. The induction motor system will be substantially more difficult to drive, since the magnetic circuit must be designed to maximize the flux in the airgap from current in the armature. Thus the inductance of the armature winding will be significantly higher, and the mutual inductance between windings will not be negligible. The results of this work will be reported at a later date.

7 Conclusions

The initial conclusion is that the PM machine is a very good solution, being surprisingly small and simple, with a manageable power electronics switching system. The superconducting machine does not appear to provide sufficient advantage to make the extra complexity worthwhile, unless weight becomes a much more significant concern than has so far appeared. However there will be advantages in the power electronic system. The induction machine design will be very complex, and the cost of the power electronics is liable to be substantially higher because of the much higher inductances.

8 Acknowledgments

This work was supported by the US Office of Naval Research (ONR) under grant N00014-1-0131.

9 References

1 R. Dougal, T. Lovett, A. Monti, E. Santi "A Multilanguage Environment for Interactive Simulation and Development of Controls for Power Electronics", IEEE Power Electronics Specialists Conference, Vancouver, Canada, June 17-22, 2001.

2 S. Yamamura, "Theory of linear induction motors", John Wiley and Sons, 1972

3 I. Boldea, S. A. Nasar, "Linear Motion Electromagnetic Systems", John Wiley and Sons, 1985

4 I. Boldea, S. A. Nasar, "Linear Electric Motors: Theory, Design and Practical Applications", Prentice-Hall, 1987

5 S. C. Ahn, J. H. Lee, D. S. Hyun, "Dynamic Characteristic Analysis of LIM Using Coupled FEM and Control Algorithm" IEEE Transactions on Magnetics, vol. 36, No. 4, July 2000, pp. 1876-1880

6 K. Davey "Pulsed Linear Induction Motors In Maglev Applications" IEEE Transactions on Magnetics, vol. 36, No. 5, September 2000, pp. 3703-3705

7 J. Faiz, H. Jafari, "Accurate Modeling of Single-Sided Linear Induction Motor Considers End Effect and Equivalent Thickness" IEEE Transactions on Magnetics, vol. 36, No. 5, September 2000, pp. 3785-3790

8 "A wound Rotor Motor 1400 Feet Long" Westinghouse Engineer, September 1946, P160-161.

9 http://historia.et.tudelft.nl/pub/art/machines.php3#III3

10 T J E Miller Brushless, Permanent-Magnet and Reluctance Motor Drives, OUP 1989.

11 Chunting Mi, Gordon R. Slemon and Richard Bonert, "Modeling of Iron Losses of Surface-Mounted Permanent Magnet Synchronous Motors", Record of the 36th Annual IEEE Industry Applications Society Conference, IAS '2001 Chicago, October 2001.

12 I. Boldea, S. A. Nasar, Linear Electric Actuators and Generators, Cambridge University Press, 1997